

<https://doi.org/10.1038/s41538-025-00414-x>

# The fine structure of starch: a review

Check for updates

**Chen Zhiguang<sup>1</sup>, Zhong Haixia<sup>1,2</sup>✉, Chen Min<sup>1</sup>, Gong Fayong<sup>1</sup>✉ & Li Jing<sup>1</sup>✉**

Starch is an important renewable resource in nature. In this paper, the recent research advances in starch structure were systematically summarized from the granular and molecular levels. Meanwhile, the changes in starch multi-scale structures under different conditions were discussed. Furthermore, we redefine the growth ring structure of starch granule, and postulate a model for the fine structure of starch granule. It may provide important insights for the research of starch.

Starch is one of the most important renewable resources in nature, with extensive applications in various fields, including food, feed, biology, medicine, materials, and chemicals<sup>1</sup>. The determination of its applications is contingent upon its properties, which in turn are determined by the underlying structure. An in-depth understanding of the intrinsic structure of starch is thus important to understand the changes in its properties during processing.

The fine structure of starch is one of the major challenges that have plagued starch researchers in recent decades. Many researchers have been devoted to the study of starch multi-scale structures, including granule structure, growth ring structure, and molecular structure of starch, etc. In addition, many scholars, such as Eric, Apriyanto, Seung, Wang, and Copeland, etc. have summarized the progress of research on starch structure<sup>2-5</sup>. These studies and papers have contributed greatly to the elucidation of the fine structure of starch.

With the continuous development of molecular simulation and various characterization techniques, the study of starch structure has been taken to a new level in recent years. In this paper, the previous advances in the study of starch structure were summarized. And the latest findings in the study of starch structure were updated, including new insights in starch molecular conformation, hydrogen bonding distribution, shell structure, growth ring structure, etc. This paper will provide an important reference for the complete elucidation of the fine structure of starch. Meanwhile, it may provide important insights for the development and utilisation of starch.

## Molecular level

### Molecular structure: average molecular weight and chain length distribution

Starch molecules are classified into two types: amylose and amylopectin. Amylose molecule is a linear polymer consisting of 2000–12000 glucose units linked by  $\alpha$ -1,4 glycosidic bonds, with few branches. It exhibits a molecular weight of approximately  $10^6$  and has a single non-reducing end. The Amylopectin molecule is a branch-like structure based on the amylose molecule, comprising approximately 5% branches connected by  $\alpha$ -1,6 glycosidic bonds. Its molecular weight is approximately  $10^8$  (higher than that of

amylose), and it possesses numerous non-reducing ends, which makes it more susceptible to hydrolysis by  $\beta$ -amylase compared to amylose<sup>6</sup>.

The molecular structure of starch is a primary determinant of its overall structural characteristics, exerting a significant impact on its macroscopic properties. For example, colour is a very easily observable property of starch gel, after undergoing boiling water treatment, different starches were fully gelatinised, resulting in different starch gels. As shown in Supplementary Data Fig. 1, different starch gels have different colours<sup>7</sup>. The fundamental reason why different starch gels exhibit different colours is the difference in their average molecular weight and chain length distribution.

The molecular structures of different starches were analysed in our prior studies. As shown in Supplementary Data Table 1, the molecular structures (molecular weight and chain length distribution) of the different starches vary considerably<sup>7</sup>. Among them, potato starch has the highest average molecular weight at two to three times that of the other starches<sup>7</sup>. It should be noted that the starch molecular weight also varies considerably between different varieties. For example, the average molecular weights of potato starches are  $1.5 \times 10^8$ ,  $5.3 \times 10^7$  and  $9.7 \times 10^7$  in the studies of Rocha et al., Chi et al. and Fang, respectively<sup>7,9</sup>. The average molecular weights of corn starches are respectively  $4.8 \times 10^7$ ,  $1.3 \times 10^7$  and  $4.6 \times 10^7$  in different studies<sup>7,9,10</sup>. This is because different researchers used different starch varieties.

In terms of chain length distribution, the side chains of amylopectin can be classified into A-chains (DP < 12) and B-chains (DP > 12) according to the difference in polymerisation degree, where chains with DP 13–24, DP 24–36, and DP > 36 are called B1, B2, and B3 chains, respectively<sup>3</sup>. As shown in Supplementary Data Table 1, discernible variations can be seen in the chain length distributions among different starches<sup>7</sup>. In addition, the B1 chain accounts for the largest share of approximately 30% to 50%. The A chain, B2 chain and B3 chain each account for approximately 10% to 30%<sup>7,11-14</sup>.

Moreover, different processing and modification treatments have significant effects on the molecular structure of starch, as summarised in Supplementary Data Table 2. Irradiation treatment has the highest effect on the molecular structure of starch and can reduce the average molecular weight of corn starch by approximately 98.5%<sup>15,16</sup>. This is due to the free

<sup>1</sup>Panxi Crops Research and Utilization Key Laboratory of Sichuan Province, College of Agricultural Sciences, Xichang University, Xichang, Sichuan Province, 615000, China. <sup>2</sup>Qinghai Tibetan Plateau Key Laboratory of Agricultural Product Processing, Academy of Agricultural and Forestry Sciences, Qinghai University, Xichang, Qinghai Province, 810016, China. ✉e-mail: zhonghaixiaxcc@126.com; gongfayong@126.com; xcc03800022@xcc.edu.cn

radicals produced by irradiation attacking the glycosidic bonds and breaking a large number of glycosidic bonds. Moist-heating treatment can reduce the average molecular weight of starch by approximately 30%<sup>17-20</sup>, whereas high-pressure, dry-heat, and annealing treatments do not have a significant effect on the molecular structure of starch<sup>9,11,21,22</sup>.

### Molecular conformation

Starch molecular conformation refers to the spatial arrangement of atoms or groups in the starch molecule, which is dominated by non-bonding interactions, such as hydrogen bonding, van der Waals, and electrostatic interactions<sup>23</sup>. Based on the aforementioned observations, it is evident that high-pressure and annealing treatments do not have a significant effect on the molecular structure (average molecular weight and chain length distribution) of starch<sup>9,11,21,22</sup>. However, these treatments result in significant changes in the starch properties<sup>9,11,21,22</sup>. It can be speculated that the changes in starch properties after high-pressure or annealing treatments are closely related to the changes in the molecular conformation of starch.

As shown in Fig. 1, the natural starch molecule is generally assumed to have a left-hand helix conformation, according to the principle of lowest energy<sup>24</sup>. In this left-hand helical structure, each helix turn contains six glucose residues with a pitch of approximately 2.3 nm. Additionally, the angle C1-O4'-C4' and dihedral angles O5-C1-O4'-C4' and C1-O4'-C4'-C5' are 166.7°, 72.8°, and 209.3°, respectively<sup>23</sup>. In an amylopectin molecule, the angle C1-O6'-C6' and dihedral angles C1-O6'-C6'-C5' and O5-C1-O6'-C6' are 115.1°, 179.1°, and 95.2°, respectively<sup>24</sup>. In an aqueous solution, this left-handed helical structure of starch is stable, with a molecular fluctuation below 0.7 nm (calculated from RMSF values)<sup>24</sup>.

In addition, the molecular conformation of starch changes in response to changes in its external environment. As shown in Fig. 2, previous studies found that heat treatment at 100 °C bent starch molecules, shortened their pitch, and increased the interchain distance of amylopectin molecules<sup>25</sup>. High-pressure treatment at 900 MPa resulted in slight bending of the starch molecules, slight shortening of the pitch, a decrease in the interchain distance of amylopectin molecules, and a decrease in the value of Rg<sup>23,24</sup>. Treatment with 4 mol/L NaCl and MgCl<sub>2</sub> caused starch molecules to become thicker and shorter (but not curved), resulting in a significant

decrease in the pitch and Rg, increase in the internal cavity of the helix, and tight intertwining of the side chains of amylopectin molecules<sup>26,27</sup>. In an oil bath, when a triglyceride molecule is close to an amylose molecule, the amylose molecule wraps around the triglyceride molecule circle-by-circle (eight glucose residues per circle with up to three circles) to form a stable complex. After complexation, the amylose molecule changes its conformation from a left-hand helix to a V-helix, which has a small pitch and a large internal cavity<sup>28</sup>. And these conformational changes of starch molecules in different environments are closely related to changes in starch hydrogen bonding (See 2.4 Hydrogen bonding for details).

In conclusion, different environmental conditions cause significant changes in the molecular conformation of starch. These conformational changes may be closely related to changes in starch properties under these different conditions.

### Pyran ring conformation (glucose residue conformation)

As shown in Fig. 3, the glucose residues in starch molecules primarily exhibit conformations such as 4C1-chair, 1C4-chair, half-chair, boat type, and envelope type<sup>29</sup>. Naturally, approximately 97.5% of the glucose residues in starch molecules exist in the 4C1-chair conformation, which is the most stable state with the lowest free energy (approximately 5 to 10 kJ/mol). The free energy of the 1C4-chair conformation is usually approximately 10–30 kJ/mol, whereas that of others, such as chairs, boats, envelopes, or half-chairs, is usually approximately 30–50 kJ/mol<sup>30</sup>.

The conformation of glucose residues changes in response to changes in the external environment. It was found that heat treatment at 100 °C decreased the proportion of 4C1-chair conformation from 97.5% to 92.7%<sup>25</sup>. High-pressure treatment at a pressure of 900 MPa increased the proportion of 4C1-chair conformation from 97.5% to 99.8%<sup>24</sup>. Treatment with 4 mol/L of MgCl<sub>2</sub> decreased the proportion of 4C1-chair conformation from 97.5% to 87.3%<sup>27</sup>. In an oil bath, the proportion of the 4C1-chair conformation of glucose residues that did not complex with lipids decreased from 97.5% to 93.8%, whereas for glucose residues that complexed with lipids, the proportion increased from 97.5% to 99.1%<sup>28</sup>. However, it's hard to know why the conformation of the pyran ring will be different in different environments, which may need to be followed up with more in-depth exploration.

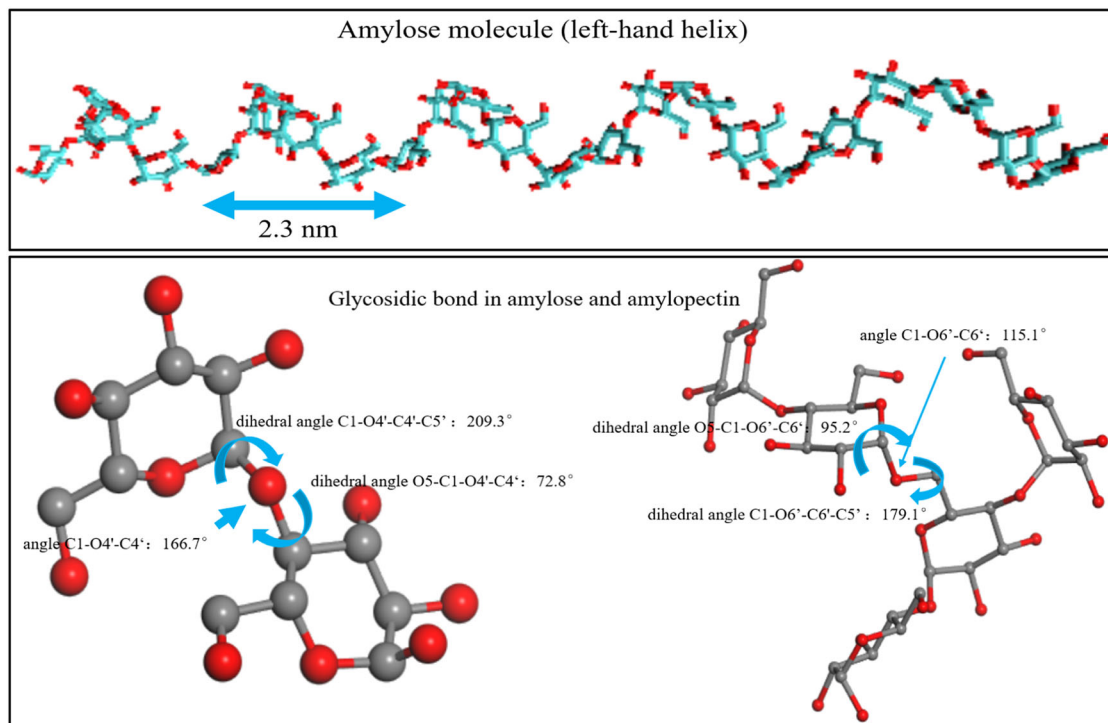
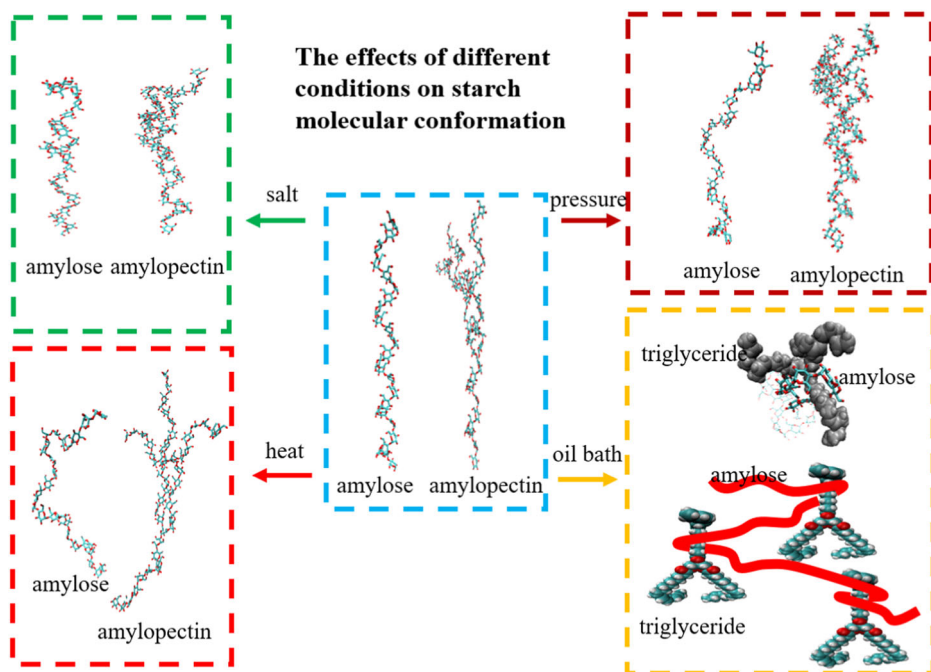
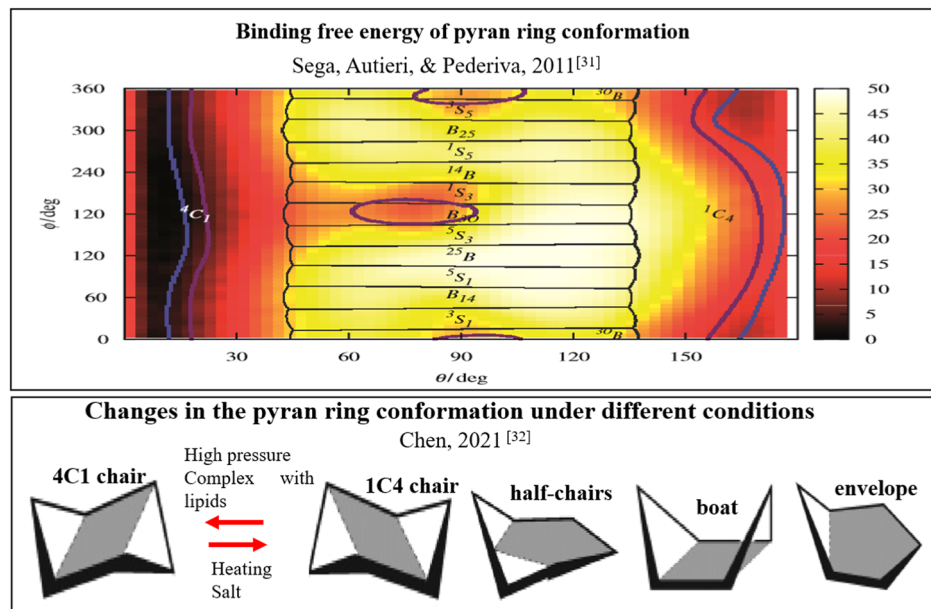


Fig. 1 | Left-hand helix amylose and glycosidic bond of starch molecules.

**Fig. 2** | Changes in starch molecular conformation under different conditions.



**Fig. 3** | Changes in the conformation of glucose residue under different conditions.



In addition, pyran ring conformational distribution can indicate that starch molecules are in different binding free energy states (molecular stability). Based on the above results, it can be understood that heating and salt treatments will increase the binding free energy of starch molecules and make starch molecules unstable. Whereas high pressure treatment and complexation with lipids reduce the binding free energy of starch molecules. However, the reason why these treatments change the binding free energy remains unknown at present.

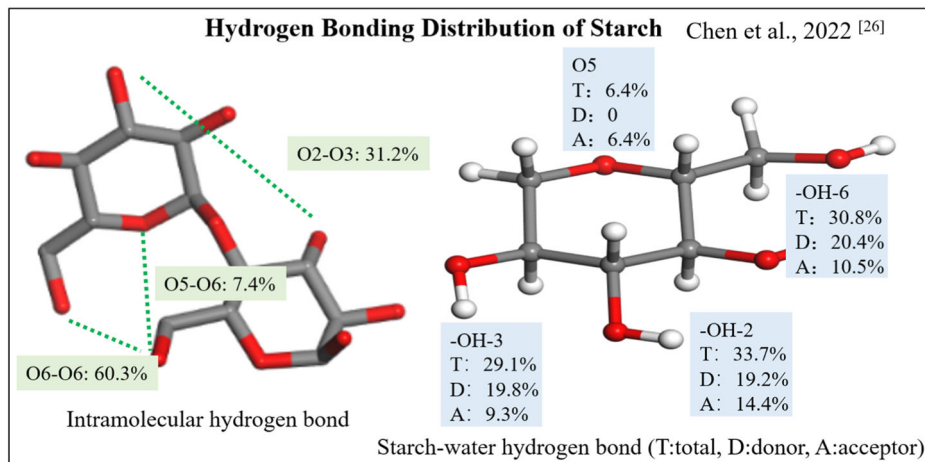
#### Hydrogen bonding

Based on the polyhydroxy structure of starch, hydrogen bonding is an important secondary interaction in starch molecules, with a bond energy of approximately 30 kJ/mol. On the one hand, because hydrogen bonding is stronger than van der Waals and electrostatic interactions, it is crucial for the

maintenance of starch structure. On the other hand, because hydrogen bonds are weaker than covalent bonds, they are more likely to break during processing, facilitating changes in the properties of starch during processing.

The distribution of hydrogen bonds in starch molecules was analysed in our previous studies<sup>25,31</sup>. As shown in Fig. 4, a single-chain starch molecule has approximately 60.3% of O6-O6 hydrogen bonds, followed by 31.2% of O2-O3 hydrogen bonds, 7.4% of O5-O6 hydrogen bonds, and only 1.1% of other hydrogen bonds, such as O2-O2 and O5-O3<sup>25</sup>. Regarding the hydrogen bonds formed between starch and water molecules, the number of starch molecules that act as hydrogen donors accounted for approximately 59.4%, which is higher than that of starch molecules acting as hydrogen acceptors<sup>25</sup>. In starch molecules, O2, O3, and O6 can act as both hydrogen donors and acceptors, whereas O5 can only act as a hydrogen acceptor<sup>25</sup>. However, starch molecules still prefer to act as hydrogen donors when

**Fig. 4** | Distribution of the hydrogen bonds in starch molecules.



forming hydrogen bonds with water molecules. Deducing the reasons for this may require more in-depth studies.

In addition, the -OH<sub>2</sub> in the starch molecule was the most likely to form hydrogen bonds with water molecules, accounting for approximately 33.7%, followed by -OH<sub>6</sub> and -OH<sub>3</sub>, accounting for 30.8% and 29.1%, respectively, whereas O<sub>5</sub> was the least likely to form hydrogen bonds with water molecules, accounting for only 6.4%<sup>31</sup>. Even when comparing only the number of hydrogen bonds that starch molecules act as hydrogen acceptors, the number of hydrogen bonds formed between O<sub>5</sub> and water (6.4%) was still lower than that for O<sub>2</sub>, O<sub>3</sub>, and O<sub>6</sub> (14.4%, 9.3%, and 10.5%, respectively)<sup>31</sup>, which may be attributed to the position of the oxygen atom in O<sub>5</sub> in the carbocyclic ring.

Moreover, the distribution of hydrogen bonds in the starch molecules changes with the external environment. The essence of starch pasting is that water molecules enter the interior of starch granules to form new hydrogen bonds with the starch hydroxyl groups, destroying the original intramolecular hydrogen bonds and freeing the starch molecules from the granules. High pressure breaks the intramolecular hydrogen bonds and promotes the formation of hydrogen bonds between starch and water. At 900 MPa, the hydration capacity of starch molecules is seen to be 165% of that at atmospheric pressure<sup>23,24</sup>. In addition, heating treatment disrupted intramolecular hydrogen bonds and inhibited the formation of hydrogen bonds between starch and water<sup>25</sup>. Furthermore, a high concentration of ions slightly increased the number of intramolecular hydrogen bonds and significantly improved the hydration capacity of starch<sup>27</sup>. For example, 4 mol/L of MgCl<sub>2</sub> increased the hydration capacity of starch molecules by 65.6 times, which is the fundamental reason for MgCl<sub>2</sub> destroying starch granules and gelatinising starch at room temperature<sup>27</sup>.

In summary, the structural aspects of starch, including its molecular structure, molecular and glucose residue conformations, and hydrogen bonding, play a crucial role in determining the changes in properties that occur during starch processing.

## Granular level

### Granular structure

Starch granules are composed of amylose and amylopectin molecules that are stacked according to specific laws. As shown in Supplementary Data Fig. 2, the morphology and granular size of starch granules exhibit significant differences depending on the plant source, with granular sizes ranging from 0.5 to 120  $\mu\text{m}$ <sup>32</sup>. Some starch granules have unique morphologies. For example, wheat starch granules exhibit two morphologies: A-type with a granular size of approximately 20  $\mu\text{m}$  and B-type with a granular size of approximately 5  $\mu\text{m}$ <sup>33</sup>. In addition, some starch granules, such as those found in corn and buckwheat, possess a distinct channel structure, as shown in Supplementary Data Fig. 2. Using laser confocal microscopy, it was observed that this channel structure links the interior to

the surface of the granules, which may be closely related to starch hydrolysis<sup>34</sup>.

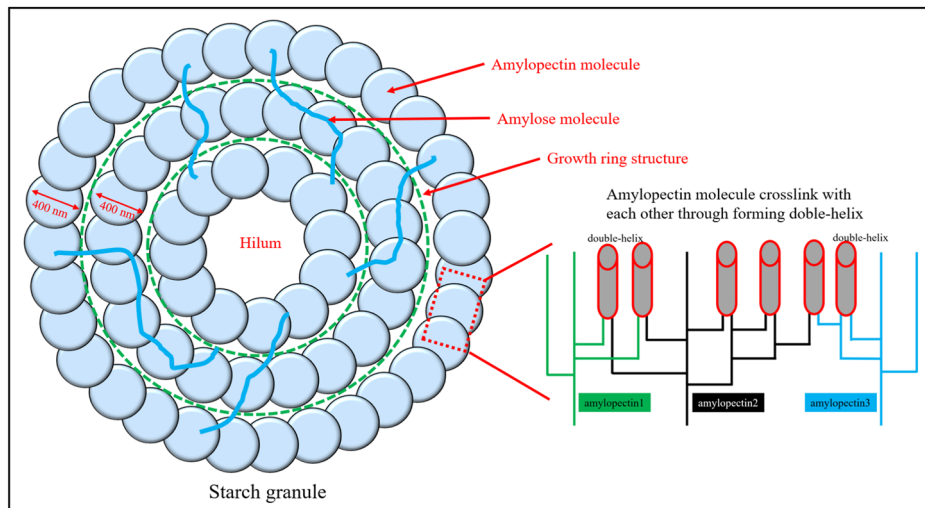
The effects of different processing and modification methods on the granular sizes of the four common starches are summarised in Supplementary Data Table 3. Dry-heating, moist-heating, annealing, and high-pressure treatments all resulted in an increase in the average granular size of the starches<sup>35–38</sup>, where the moist-heating treatment had the most pronounced effect on granular size<sup>19,39–41</sup>. During moist-heating, annealing or high-pressure treatment, starch granules absorb water and swell slightly (but are not fully pasted), which is an important reason for the increase in granular size. Dry-heating treatment will increase the intermolecular distance (see 2.2 Molecular conformation), which may be an important reason for the increase in starch granular size. In contrast, irradiation treatment breaks up large granules, leading to a decrease in average granular size<sup>42,43</sup>.

The granular structure of starch significantly affects the processing properties of grain-based foods. For example, a close relationship exists between the granular size and Carr index, which is closely related to the flowability of the powder. This determines whether rice flour, starch, etc. will stick to equipment such as conveyor belts during processing or easily clog the processing equipment. In general, the larger the particle size, the lower the Carr index, and the better the powder flowability<sup>44</sup>. Starch granular size is also related to packaging density. Thus, granular size is closely related to the quality of extruded products, such as cookies, cereals, and buckwheat tea. In addition, the granular size and degree of granule destruction (degree of gelatinisation) are closely related to solubility, swelling, water absorption, digestion rate, thermal properties, and gel texture. And these indices determine the quality of the starch products.

### Growth ring structure

As shown in Supplementary Data Fig. 3, the concentric ring-like structure was found on the starch granule profile by using SEM (scanning electron microscope), which is named the growth ring structure of starch<sup>45</sup>. And researchers generally agree that the growth ring is composed of an alternating amorphous ring and semi-crystalline ring, with a width of about 400 nm<sup>46</sup>. In one of our recent studies (Supplementary Data Fig. 4), the buckwheat starch granule was observed by using a high-resolution 3D CT with a resolution of 50 nm (Unpublished, see supplementary data). As shown in Supplementary Data Fig. 4, it was found that, the starch granule is an externally dense and internally loose (or even hollow) structure. In addition, in the results of 3D CT, higher brightness indicates higher density. And the density of the crystalline region would be significantly higher than that of the amorphous region. However, no alternating light and dark bands were found in the 3D CT (Supplementary Data Fig. 4), which suggests that the growth rings in starch granule may be not alternately amorphous and semi-crystalline, which may need more verification.

Fig. 5 | Speculation on starch granule structure.



In our previous study, it can be calculated that the starch molecule has a pitch of 2.3 nm per 6 glucose residues through energy minimization principle and molecular simulation<sup>31</sup>. Thus, the length of the main chain of an amylopectin molecule (containing 1000 glucose residues) will be about 400 nm. It can be seen that, the size of the growth ring (200–500 nm) is very close to that of an amylopectin molecule. This suggests that the growth ring structure may be composed of a ring of amylopectin molecules.

Therefore, the starch granule structure was speculated according to the above results. As shown in Fig. 5 (Each blue circle represents one amylopectin molecule), the starch granule is composed of multiple growth rings arranged layer by layer. Each growth ring measures approximately 400 nm. And the gap between each growth ring is less than 50 nm, otherwise dark bands will be observed in 3D CT scans. And the so-called “amorphous ring” observed in Supplementary Data Fig. 3 may be the gap between the growth ring (amylopectin ring). In the growth ring, neighbouring amylopectin molecules are tightly cross-linked with each other by forming double helix structures. The double helix structures ensure the relative stability of the growth ring structure. In this starch granule model, the amylopectin molecules are the key for the formation of starch granule. It is well known that the amylopectin content of waxy starches can be close to 100%, whereas the amylose content of high-amylose starches can only go up to about 60% or else the granules cannot be formed. This model of starch granule structure is also consistent with this phenomenon. How the amylose molecule is involved in the stacking of starch granules will be discussed later in the outer shell structure.

### Outer shell structure

In our previous study, numerous undamaged outer shells of starch granules were obtained after thermal treatment at temperatures lower than the pasting temperature in an acetic acid system<sup>32</sup>. At this point, the starch granule structure no longer exists, and the internal molecules separate from the granules and participate in the formation of starch gel. As shown in Supplementary Data Fig. 5, the thicknesses of the outer shells of different starches are all within 1  $\mu$ m, and the interior is hollow with almost no adherents. It can be hypothesised that the outer shell of starch granules is denser than the inner shell, which makes it easier to maintain its original morphology when subjected to external forces<sup>47</sup>.

In the starch granule model (Fig. 5), the amylose molecules may traverse multiple growth rings, distributed throughout the starch granules. Studies showed that the higher the amylose content, the higher the gelatinization temperature of starch<sup>48</sup>. This suggests that amylose molecules can cross-link with the amylopectin molecules from different growth rings (like a rope binding multiple growth rings), which in turn prevents the granules from expanding. That is, the amount of amylose determines the stability between different growth rings.

The outer shells of starch granules were obtained and the amylose content was detected by Yang et al.<sup>32</sup>. It was found that the amylose content in outer shells was higher than in the whole granule<sup>32</sup>. Thus, it can explain why the outer shell of granule is more stable than the inner structure. A large number of amylose molecules are distributed at the outer shell of the granule and making the growth rings at the periphery of the granule more tightly cross-linked with each other.

### Crystalline structure

**Crystalline type and relative crystallinity.** The relative crystallinities of different starches generally range from 10 to 45%<sup>3</sup>. Based on X-ray diffraction results, starch can be classified into four crystalline types: A, B, C, and V type. Crystalline diffraction peaks for A type appeared at 15°, 17°, 18°, and 23°. Crystalline diffraction peaks for B type appeared at 5.6°, 17°, 22°, and 24°. C-type crystals were a mixture of the A and B types. The V type exhibited special diffraction peaks formed after the interactions of starch molecules with lipids, iodine, or other small molecules.

The effects of different processing and modification methods on the relative crystallinity and crystalline type of starch are summarised in Supplementary Data Table 4. It can be seen that the moist-heating treatment decreased the relative crystallinity of starch and could change the B type to C type<sup>17–19</sup>. The high-pressure treatment caused a significant decrease in the relative crystallinity and changed the A-type to B type<sup>38,49,50</sup>. In contrast, irradiation, annealing, and dry heating treatments had less effect on the relative crystallinity and no effect on the crystalline type<sup>51–53</sup>.

Both the crystalline type and relative crystallinity significantly affect the macroscopic properties of starch. For example, with little difference in relative crystallinity, B-type crystals (e.g., potato starch) are more resistant to high pressure than A-type crystals (e.g., corn starch)<sup>38</sup>. The reason why B-type crystal is more resistant to high pressure than A-type crystal is that, the structure of A-type crystal is denser than the structure of B-type crystal (Supplementary Data Fig. 6). The key to high-pressure induced starch gelatinisation is the pressure difference between the inside and outside. During high-pressure treatment of starch, high-pressure treatment promotes starch hydration. And the dense A type crystals are more likely to be clogged by water molecules entering the granules, then the structure disintegrates under the pressure difference between the inside and outside<sup>54</sup>. In contrast, A-type crystals are more resistant to heat, acids, and bases than B-type crystals<sup>35</sup>. Starches with high relative crystallinity are generally accepted to be more resistant and exhibit slower digestion rates.

**Crystalline lamellae.** As mentioned above, it suggests that the growth rings in starch granule are not alternately amorphous and semi-crystalline. It is important to note that this result does not contradict

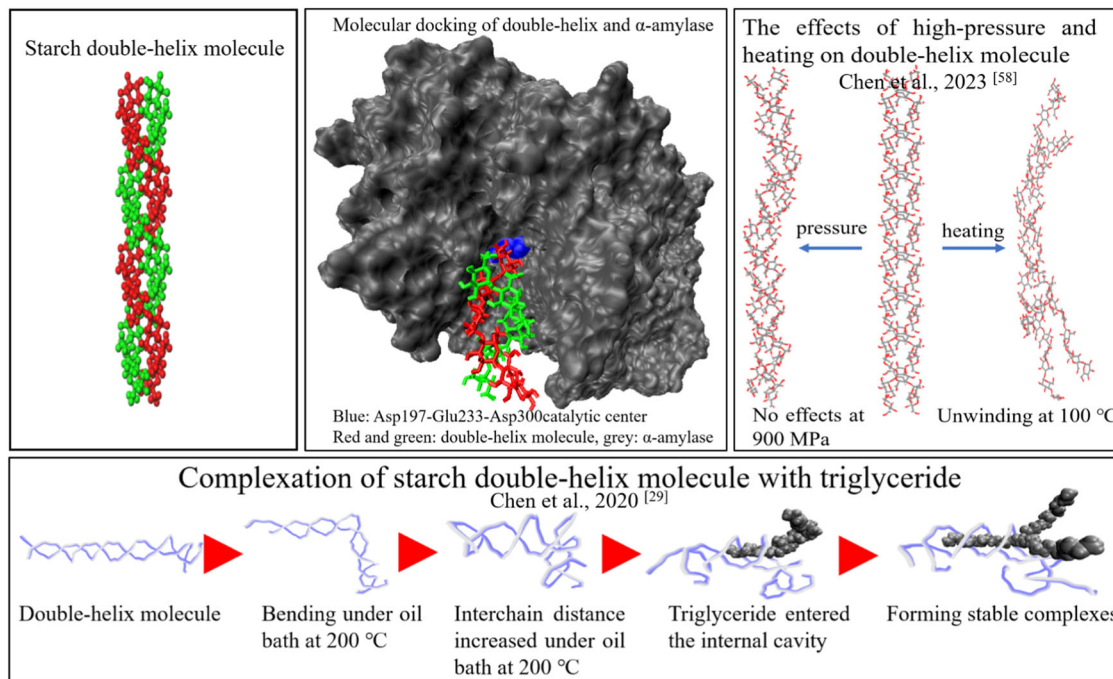


**Fig. 6** | Starch double-helix structure and its changes under heat, high pressure, and oil bath; molecular docking of  $\alpha$ -amylase and double-helix.

the theory of crystalline lamellae. Crystalline lamellae are composed of regularly arranged double helices formed by the side chains of amylopectin molecules. The repeat distance of semi-crystalline lamellae was calculated using small-angle X-ray diffraction to be approximately 9–10 nm<sup>56</sup>. The thicknesses of the amorphous and crystalline lamellae were approximately 3 and 6 nm, respectively<sup>56</sup>. Using molecular simulations, it was calculated that the head-to-tail distance of a double-helix structure consisting of two amylose molecules containing 18 glucose residues is approximately 6 nm when fully extended<sup>24</sup>, which suggests that the double-helix structure in the crystalline lamellae needs to consist of two side chains with 18 (or more) glucose residues. In addition, the results of the chain length distribution showed that the proportion of the side chains with DP > 18 was approximately 50%<sup>7</sup>.

Moreover, two hypotheses exist regarding the stacking forms of the crystalline lamellae: the cluster model and the building block backbone model<sup>57</sup>. As shown in Supplementary Data Fig. 6, the biggest difference between the two models is the orientation of the side chains in the amylopectin molecules (or  $\alpha$ -1,6-glycosidic bond angles). In our previous study, amylopectin was energetically minimised until its conformation was stabilised. Subsequently, it was found that the angle C1-O6'-C6' and dihedral angles C1-O6'-C6'-C5' and O5-C1-O6'-C6' of the amylopectin molecule were 115.1°, 179.1°, and 95.2°, respectively<sup>23,24</sup>. The conformations with these angles are more consistent with those of the cluster model.

**Double-helix structure.** The double-helix structure is the most basic unit of starch crystallisation. As shown in Fig. 6, in the double-helix structure, the average distance between the two chains is approximately 0.7 nm. The double helix is in a stable conformation, and its structural stability is maintained mainly by hydrogen bonding (mainly O2-O6 hydrogen bonding of the corresponding residues) and van der Waals forces (each pair of residues can contribute van der Waals forces of approximately 30 kJ/mol)<sup>24</sup>. For example, as previously demonstrated,  $MgCl_2$  treatment reduced the 4C1-chair conformation from 97.5% to 87.4% in amylose molecules, whereas in the double-helix structure, the proportion of 4C1-chair conformation was reduced to only 96.0% after  $MgCl_2$  treatment<sup>27</sup>.

In addition, it was found that the 900 MPa high-pressure treatment could not directly destroy the double-helix structure, while the 100 °C

heating could make the double-helix structure begin to deconvolute (Fig. 6)<sup>25</sup>. As shown in Supplementary Data Table 4, the relative crystallinity of starch was significantly reduced after high-pressure treatment, while the double-helix structure could not be destroyed, suggesting that the key to disrupting starch crystallisation by high pressure is to disrupt the regular arrangement of the double helix rather than directly disrupting the double-helix structure<sup>55</sup>.

Moreover, the double-helix structure in an oil bath can form complexes with triglyceride molecules. As shown in Fig. 6, in a previous study, the complexation process between a double-helix molecule and a triglyceride molecule was analysed using molecular simulations<sup>28</sup>. First, the interchain distance of the double helix increased in the presence of high temperatures; then, the double-helix structure bent; and finally, the triglyceride molecules were inserted into the interior of the helix at the bend to form a stable complex. This suggests that the crystalline region of starch granules can also adsorb lipids<sup>28</sup>.

Furthermore, in a previous study, molecular docking between  $\alpha$ -amylase and a double-helix molecule was performed. It was found that the double-helix molecule could not dock to the active centre of  $\alpha$ -amylase due to the spatial site-blocking effect (Fig. 6), indicating that the enzymatic efficiency of the double-helix structure would be extremely low<sup>58</sup>. This also proved that the higher the relative crystallinity of starch, the higher the content of resistant starch.

## Conclusion

In this paper, the recent research advances in starch structure were systematically summarized from the granular (granular structure, outer shell structure, growth ring structure, crystalline structure, and double-helix structure) and molecular (molecular structure, molecular conformation, pyran ring conformation, and hydrogen bonding) levels. Meanwhile, the changes in starch multi-scale structures under different conditions were discussed. Furthermore, in this paper, we redefine the growth ring structure of starch granule, and postulate a model for the fine structure of starch granule. It may provide important insights for the development and utilisation of starch.

However, owing to the limitations of characterisation, several questions regarding the fine structure of starch still remain, necessitating further investigation and validation. For example, the formation of the channel

structure and its physiological function; whether amylose molecules are involved in the construction of crystalline regions. In addition, the model of starch granule proposed in this paper also needs to be validated in subsequent studies.

In recent years, with the advancement of technology, more and more new technologies can be used for the study of starch granule structure, such as molecular dynamics simulation, high-resolution 3D CT, cryo-electron microscopy. It is believed that, in the near future, the fine structure of starch and its changes in different environments will be fully elucidated.

## Data availability

No datasets were generated or analysed during the current study.

Received: 21 October 2024; Accepted: 27 March 2025;

Published online: 11 April 2025

## References

1. Bangar, S. P., Ashogbon, A. O., Singh, A., Chaudhary, V. & Swhiteside, W. S. Enzymatic modification of starch: A green approach for starch applications. *Carbohydr. Polym.* **287**, 119265 (2022).
2. Apriyanto, A., Compart, J. & Fettke, J. A review of starch, a unique biopolymer - Structure, metabolism and in planta modifications. *Plant Sci.* **318**, 111223 (2022).
3. Eric, B. Understanding Starch Structure: Recent Progress. *Agronomy* **7**, 7030056 (2017).
4. Seung, D. Amylose in starch: towards an understanding of biosynthesis, structure and function. *N. Phytol.* **228**, 1490–1504 (2020).
5. Wang, S. J. & Copeland, L. Effect of Acid Hydrolysis on Starch Structure and Functionality: A Review. *Crit. Rev. Food Sci. Nutr.* **55**, 1081–1097 (2015).
6. Eric, B. et al. Small differences in amylopectin fine structure may explain large functional differences of starch. *Carbohydr. Polym.* **140**, 113–121 (2016).
7. Fang, C. L. *Characteristic Properties and Molecular Structures of Three Amorphous Starches of Different Shapes*. Doctoral thesis, Shaanxi Univ. Science and Technology. (2020) (In Chinese).
8. Rocha, T. S., Cunha, V. A. G., Jane, J. & Franco, C. M. L. Structural Characterization of Peruvian Carrot (*Arracacia xanthorrhiza*) Starch and the Effect of Annealing on Its Semicrystalline Structure. *J. Agric. Food Chem.* **59**, 4208–4216 (2011).
9. Chi, C. et al. Dry heating and annealing treatment synergistically modulate starch structure and digestibility. *Int. J. Biol. Macromol.* **137**, 554–561 (2019).
10. Rocha, T. S., Felizardo, S. G., Jane, J. & Franco, C. M. L. Effect of annealing on the semicrystalline structure of normal and waxy corn starches. *Food Hydrocoll.* **29**, 93–99 (2012).
11. Su, C. et al. Changes in structural, physicochemical, and digestive properties of normal and waxy wheat starch during repeated and continuous annealing. *Carbohydr. Polym.* **247**, 116675 (2020).
12. Simsek, S., Ovando-Martínez, M., Whitney, K. & Bello-Pérez, L. A. Effect of acetylation, oxidation and annealing on physicochemical properties of bean starch. *Food Chem.* **134**, 1796–1803 (2012).
13. Singh, H., Chang, Y. H., Lin, J.-H., Singh, N. & Singh, N. Influence of heat-moisture treatment and annealing on functional properties of sorghum starch. *Food Res. Int.* **44**, 2949–2954 (2011).
14. Chang, R., Lu, H., Bian, X., Tian, Y., & Jin, Z. Ultrasound assisted annealing production of resistant starches type 3 from fractionated debranched starch: Structural characterization and in-vitro digestibility. *Food Hydrocoll.* **110**, 106141 (2020).
15. Bao, J., Ao, Z. & Jane, J. Characterization of Physical Properties of Flour and Starch Obtained from Gamma-Irradiated White Rice. *Starch – Stärke* **57**, 480–487 (2005).
16. Zhou, X., Ye, X. J., He, J., Wang, R. & Jin, Z. Y. Effects of electron beam irradiation on the properties of waxy maize starch and its films. *Int. J. Biol. Macromol.* **151**, 239–246 (2020).
17. Zhang, B. et al. The molecular structure, morphology, and physicochemical property and digestibility of potato starch after repeated and continuous heat-moisture treatment. *J. Food Sci.* **85**, 4215–4224 (2020).
18. Zhang, B. et al. Comparing the multi-scale structure, physicochemical properties and digestibility of wheat A- and B-starch with repeated versus continuous heat-moisture treatment. *Int. J. Biol. Macromol.* **163**, 519–528 (2020).
19. Wang, H. et al. Insights into the multi-scale structure and digestibility of heat-moisture treated rice starch. *Food Chem.* **242**, 323–329 (2018).
20. Wang, H., Zhang, B., Chen, L. & Li, X. Understanding the structure and digestibility of heat-moisture treated starch. *Int. J. Biol. Macromol.* **88**, 1–8 (2016).
21. Zhang, B. et al. The influence of repeated versus continuous dry-heating on the performance of wheat starch with different amylose content. *LWT* **136**, 110380 (2021).
22. Szwengiel, A., Lewandowicz, G., Gorecki, A. R. & Blaszcak, W. The effect of high hydrostatic pressure treatment on the molecular structure of starches with different amylose content. *Food Chem.* **240**, 51–58 (2018).
23. Chen, Z. G. et al. The analysis of the effects of high hydrostatic pressure (HHP) on amylose molecular conformation at atomic level based on molecular dynamics simulation. *Food Chem.* **327**, 127047 (2020).
24. Chen, Z. G., Huang, J. R., Pu, H. Y. H., Yang, Q. & Fang, C. L. The effects of HHP (high hydrostatic pressure) on the interchain interaction and the conformation of amylopectin and double-amylose molecules. *Int. J. Biol. Macromol.* **155**, 91–102 (2020).
25. Chen, Z. G., Huang, J. R., Pu, H. Y. & Keipper, H. W. The Effects of temperature on starch molecular conformation and hydrogen bonding. *Starch* **74**, 2100288 (2022).
26. Chen, Z. G. et al. The effects of NaCl on starch molecular conformation. *Starch* **75**, 2200243 (2023).
27. Zhong, H. X., Chen, Z. G., Huang, J. R. & Pu, H. Y. Exploration of the process and mechanism of magnesium chloride induced starch gelatinization. *Int. J. Biol. Macromol.* **205**, 8–127 (2022).
28. Chen, Z. G. et al. Analysis of the complexation process between starch molecules and trilinolenin. *Int. J. Biol. Macromol.* **165**, 44–49 (2020).
29. Anthony, D. H. & Peter, J. R. Puckering Coordinates of Monocyclic Rings by Triangular Decomposition[J]. *Chem. Inf. Model* **47**, 1031–1035 (2007).
30. Sega, M., Autieri, E. & Pederiva, F. Pickett angles and Cremer-Pople coordinates as collective variables for the enhanced sampling of six-membered ring conformations. *Mol. Phys.* **1**, 141–148 (2011).
31. Chen, Z. G. *Study on the Change Rules of Starch Molecular Conformation and Secondary Interaction under Different Processing Conditions*. Doctoral thesis, Shaanxi Univ. Science and Technology. (2021) (In Chinese).
32. Yang, Q., Huang, J. R. & Yan, Q. The separation and characterization of starch outer shell. *Trans. Chin. Soc. Agric. Mach* **11**, 67–73 (2020). (In Chinese).
33. Huang, J., Wang, Z., Fan, L. & Ma, S. A review of wheat starch analyses: Methods, techniques, structure and function. *Int. J. Biol. Macromol.* **203**, 130–142 (2022).
34. Bae, J. E. et al. Impact of starch granule-associated surface and channel proteins on physicochemical properties of corn and rice starches. *Carbohydr. Polym.* **250**, 116908 (2020).
35. Maniglia, B. C. et al. Dry heating treatment: a potential tool to improve the wheat starch properties for 3D food printing application. *Food Res. Int.* **137**, 109731 (2020).
36. Zhu, P. et al. Morphological and physicochemical properties of rice starch dry heated with whey protein isolate. *Food Hydrocoll.* **109**, 106091 (2020).

37. Zhong, Y. et al. Microwave pretreatment promotes the annealing modification of rice starch. *Food Chem.* **304**, 125432 (2020).

38. Bajaj, R., Singh, N., Ghuman, A., Kaur, A., & Mishra, H. N. Effect of HHP Treatment on Structural, Functional, and In-Vitro Digestibility of Starches from Tubers, Cereals, and Beans. *Starch* **70**, 2100096 (2021).

39. Zhou, S. et al. Effect of heat-moisture treatment on the in vitro digestibility and physicochemical properties of starch-hydrocolloid complexes. *Food Hydrocoll.* **104**, 105736 (2020).

40. Hong, J., Li, L., Liu, C., Zheng, X. & Bian, K. Effect of Heat-Moisture Treatment on Physicochemical, Thermal, Morphological, and Structural Properties of Mechanically Activated Large A- and Small B-Wheat Starch Granules. *J. Food Sci.* **84**, 2795–2814 (2019).

41. De Oliveira, C. S. et al. Heat-moisture treatment (HMT) on blends from potato starch (PS) and sweet potato starch (SPS). *J. Therm. Anal. Calorim.* **133**, 1491–1498 (2018).

42. Teixeira, B. S., Garcia, R. H. L., Takinami, P. Y. L. & Mastro, N. L. D. Comparison of gamma radiation effects on natural corn and potato starches and modified cassava starch. *Radiat. Phys. Chem.* **142**, 44–49 (2018).

43. Li, G. T. & Zhu, F. Effect of HHP on rheological and thermal properties of quinoa and maize starches. *Food Chem.* **241**, 380–386 (2018).

44. Bangar, S. P., Kumar, M., Whiteside, W. S., Tomar, M. & Kennedy, J. F. Litchi (*Litchi chinensis*) seed starch: Structure, properties, and applications - A review. *Carbohydr. Polym. Technol. Appl.* **2**, 100080 (2021).

45. Emma, P. & Alison, M. S. Growth Ring Formation in the Starch Granules of Potato Tubers. *Plant Physiol.* **123**, 365–371 (2003).

46. Xu, H. B. et al. Methods for characterizing the structure of starch in relation to its applications: a comprehensive review. *Crit. Rev. Food Sci. Nutr.* **63**, 4799–4816 (2023).

47. Hu, J. et al. Outer shell, inner blocklets, and granule architecture of potato starch[J]. *Carbohydr. Polym.* **103**, 355–358 (2014).

48. Sandhu, K. S., Kaur, M., Singh, N. & Lim, S. T. A comparison of native and oxidized normal and waxy corn starches: Physicochemical, thermal, morphological and pasting properties. *LWT - Food Sci. Technol.* **41**, 1000–1010 (2008).

49. Zeng, F., Li, T., Gao, Q. Y., Liu, B. & Yu, S. J. Physic ochemical properties and in vitro digestibility of high hydrostatic pressure treated waxy rice starch. *Int. J. Biol. Macromol.* **120**, 1030–1038 (2018).

50. Colussi, R. et al. HHP processing and retrogradation of potato starch: Influence on functional properties and gastro-small intestinal digestion in vitro. *Food Hydrocoll.* **75**, 131–137 (2018).

51. González, M., Vernon-Carter, E. J., Alvarez-Ramirez, J. & Carrera-Tarela, Y. Effects of dry heat treatment temperature on the structure of wheat flour and starch in vitro digestibility of bread. *Int. J. Biol. Macromol.* **11**, 1439–1447 (2020).

52. Zhong, Y. Y. et al. High-amylose starch: Structure, functionality and applications. *Crit. Rev. Food Sci. Nutr.* **63**, 8568–8590 (2022).

53. Zhou, W. et al. The impacts of particle size on starch structural characteristics and oil-binding ability of rice flour subjected to dry heating treatment. *Carbohydr. Polym.* **223**, 115053 (2019).

54. Chen, Z. G., Yang, Q., Yang, Y. S. & Zhong, H. X. The effects of high-pressure treatment on the structure, physicochemical properties and digestive property of starch. *Int. J. Biol. Macromol.* **244**, 125376 (2023).

55. Chen, Z. G., Yao, Y., Pu, H. Y., Huang, J. R. & Zhong, H. X. The effects of high-pressure treatment on starch pasting, retrogradation, thermal, crystalline, rheological and digestive properties – A review. *Int. J. Food Sci. Technol.* **58**, 2189–2198 (2023).

56. Cardoso, M. & Westfahl, H. H. On the lamellar width distributions of starch[J]. *Carbohydr. Polym.* **81**, 21–28 (2010).

57. Eric, B. On the Building Block and Backbone Concepts of Amylopectin Structure. *Cereal Chem.* **90**, 294–311 (2013).

58. Zhong, H. X. et al. Analysis of the interaction between double-helix starch molecule and  $\alpha$ -amylase. *Innov. Food Sci. Emerg. Technol.* **94**, 103658 (2024).

## Acknowledgements

This work is supported by the Open Project Program of Panxi Crops Research and Utilization Key Laboratory of Sichuan Province (No. SZ22ZZ01) and the Project of Xichang University (No. YBZ202212).

## Author contributions

Chen Zhiguang and Zhong Haixia: Writing—review & editing; Writing—original draft. Chen Zhiguang and Chen Min.: Literature searching. Gong Fayong and Li Jing: Writing—review & editing.

## Competing interests

The authors declare no competing interests.

## Additional information

**Supplementary information** The online version contains supplementary material available at <https://doi.org/10.1038/s41538-025-00414-x>.

**Correspondence** and requests for materials should be addressed to Zhong Haixia, Gong Fayong or Li Jing.

**Reprints and permissions information** is available at <http://www.nature.com/reprints>

**Publisher's note** Springer Nature remains neutral with regard to jurisdictional claims in published maps and institutional affiliations.

**Open Access** This article is licensed under a Creative Commons Attribution-NonCommercial-NoDerivatives 4.0 International License, which permits any non-commercial use, sharing, distribution and reproduction in any medium or format, as long as you give appropriate credit to the original author(s) and the source, provide a link to the Creative Commons licence, and indicate if you modified the licensed material. You do not have permission under this licence to share adapted material derived from this article or parts of it. The images or other third party material in this article are included in the article's Creative Commons licence, unless indicated otherwise in a credit line to the material. If material is not included in the article's Creative Commons licence and your intended use is not permitted by statutory regulation or exceeds the permitted use, you will need to obtain permission directly from the copyright holder. To view a copy of this licence, visit <http://creativecommons.org/licenses/by-nc-nd/4.0/>.

© The Author(s) 2025